# REPORT DOCUMENTATION PAGE

Form Approved
OMB NO. 0704-0188



| 1. AGENCY USE ONLY (Leave blank) | 2. REPORT DATE | 3. REPORT TYPE AND DATES COVERED |
|---|---|---|
| | March 12, 2001 | June 1, 1999 - December 31, 2000 **FINAL** |

**4. TITLE AND SUBTITLE**
Mid-Infrared Laser Phosphors

**5. FUNDING NUMBERS**
DAAD-19-99-1-0229

**6. AUTHOR(S)**
S.C. Rand

**7. PERFORMING ORGANIZATION NAME(S) AND ADDRESS(ES)**
University of Michigan, Dept. of EECS
1301 Beal Avenue, 1112 EECS
Ann Arbor, MI 48109-2122

**8. PERFORMING ORGANIZATION REPORT NUMBER**

**9. SPONSORING / MONITORING AGENCY NAMES(S) AND ADDRESS(ES)**
U.S. Army Research Office
P.O. Box 12211
Research Triangle Park, NC 27709-2211

**10. SPONSORING / MONITORING AGENCY REPORT NUMBER**
39881-PH
.7

**11. SUPLEMENTARY NOTES**
The views, opinions and/or findings contained in this report are those of the author(s) and should not be construed as an official Department of the Army position, policy or decision, unless so designated by other documentation.

**12a. DISTRIBUTION / AVAILABILITY STATEMENT**
Approved for public release; distribution unlimited.

**12b. DISTRIBUTION CODE**
A

**13. ABSTRACT (Maximum 200 words)**
The main goal of this project was to investigate *doped nanodielectrics* as optical materials in which strong scattering conditions offer prospects of laser phosphors and uniquely intense mid-infrared light sources. The one year effort on this project was expected to provide new materials for this purpose and to analyze their emission properties for evidence of stimulated emission at a preliminary level. Most of the main objectives were achieved within the project period, as described in this report. In particular, continuous-wave laser action was demonstrated in electrically-pumped nanophosphors.

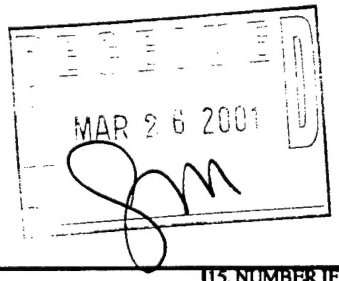


| 14. SUBJECT TERMS | 15. NUMBER IF PAGES |
|---|---|
| Nanodielectrics, nanophosphors | 16 |
| | 16. PRICE CODE |

| 17. SECURITY CLASSIFICATION OR REPORT | 18. SECURITY CLASSIFICATION OF THIS PAGE | 19. SECURITY CLASSIFICATION OF ABSTRACT | 20. LIMITATION OF ABSTRACT |
|---|---|---|---|
| **UNCLASSIFIED** | **UNCLASSIFIED** | **UNCLASSIFIED** | **UL** |

NSN 7540-01-280-5500

Standard Form 298 (rev. 2-89)
Prescribed by ANSI Std. 239-18
298-102

20010413 076

MEMORANDUM OF TRANSMITTAL

To: U. S. Army Research Office
Attn: AMSRL-RO-BI (TR)
P.O. Box 12211
Research Triangle Park, NC 27709-2211

Date 3/12/01

_____ Reprint (Orig + 2 copies)

_____ Technical Report (Orig + 2 copies)

_____ Manuscript (1 copy)

__X__ Final Progress Report (Orig + 2 copies)

_____ Related Materials, Abstracts, Thesis (1 copy)

CONTRACT/GRANT NUMBER: DAAD19-99-1-0229

REPORT TITLE: FINAL Technical Report: Mid-Infrared Laser Phosphors

is forwarded for your information.

SUBMITTED FOR PUBLICATION TO (applicable only if report is manuscript):

Sincerely,

Stephen Rand
University of Michigan
1301 Beal Avenue
1108 EECS Bldg
Ann Arbor, MI 48109-2122

# Final Technical Report
## on
## "Mid-Infrared Laser Phosphors"
(U.S. DOD-Army grant DAAD19-99-1-0229)

Table of Contents

## Final Technical Report

### I. Introduction

The main goal of this project was to investigate *doped nanodielectrics* as optical materials in which strong scattering conditions offer prospects of laser phosphors and uniquely intense mid-infrared light sources. The one year effort on this project was expected to provide new materials for this purpose and to analyze their emission properties for evidence of stimulated emission at a preliminary level. Most of the main objectives were achieved within the project period, as described in this report. In particular, continuous-wave laser action was demonstrated in electrically-pumped nanophosphors.

### II. Experiments

As proposed in our original statement of work, several new nanodielectric powders were synthesized during the initial phase of the project for the investigation of mid-infrared (MIR) laser action under electrical stimulation. Using flame spray pyrolysis of low-cost ingredients, samples of alumina and yttria nanoparticles were prepared with an average grain size of 30 nm at rates up to 250 g/hr. Through the use of metallo-organic precursors, powders were prepared with a variety of dopants including Pr, Nd, Gd, Tb, Er, Tm, in concentrations ranging from 0.1-6% by weight of the rare earth ions. Samples with ~1% $Nd^{3+}$, $Gd^{3+}$ and $Pr^{3+}$ were studied the most. These materials were fully characterized by TEM, BET analysis, and x-ray diffraction and found to be predominantly non-necked single crystals that did not agglomerate (see Fig. 1). Coherent back-scattering (CBS) measurements were undertaken to reveal two things: (i) that absorption was negligible in the powders, and (ii) that the mean transport distance for light was consistently less than half a wavelength throughout the visible spectral region. Measurements (described in more detail in the next section) indicated that our materials produce exceptionally effective scattering together with low absorption and are therefore suitable for stimulated emission studies at 3.5 and 5 μm, the MIR transition wavelengths of interest in Gd and Pr respectively.

As part of the setup for MIR luminescence experiments, a 1-meter Jarrell-Ash spectrometer was outfitted with new slit, grating and detector assemblies. An UHV chamber was adapted for mid-infrared use by the installation of calcium fluoride windows. Anticipating the need to develop quick sample transfer capability between the UHV chamber and the laboratory, a new 12-inch diameter chamber and load-lock facility was designed and ordered. Both the existing six-way cross and the new chamber will be serviced by high current, high voltage electron guns to excite new phosphor materials.

Cathodoluminescent (CL) spectra were recorded with the grating spectrometer by mounting powder samples in a UHV chamber equipped with an electron gun and VIS-IR-transmitting optical ports. At room temperature, extensive sets of spectra were recorded at modest (μA) electron currents and various voltages in samples of $Nd^{3+}$:δ-$Al_2O_3$,

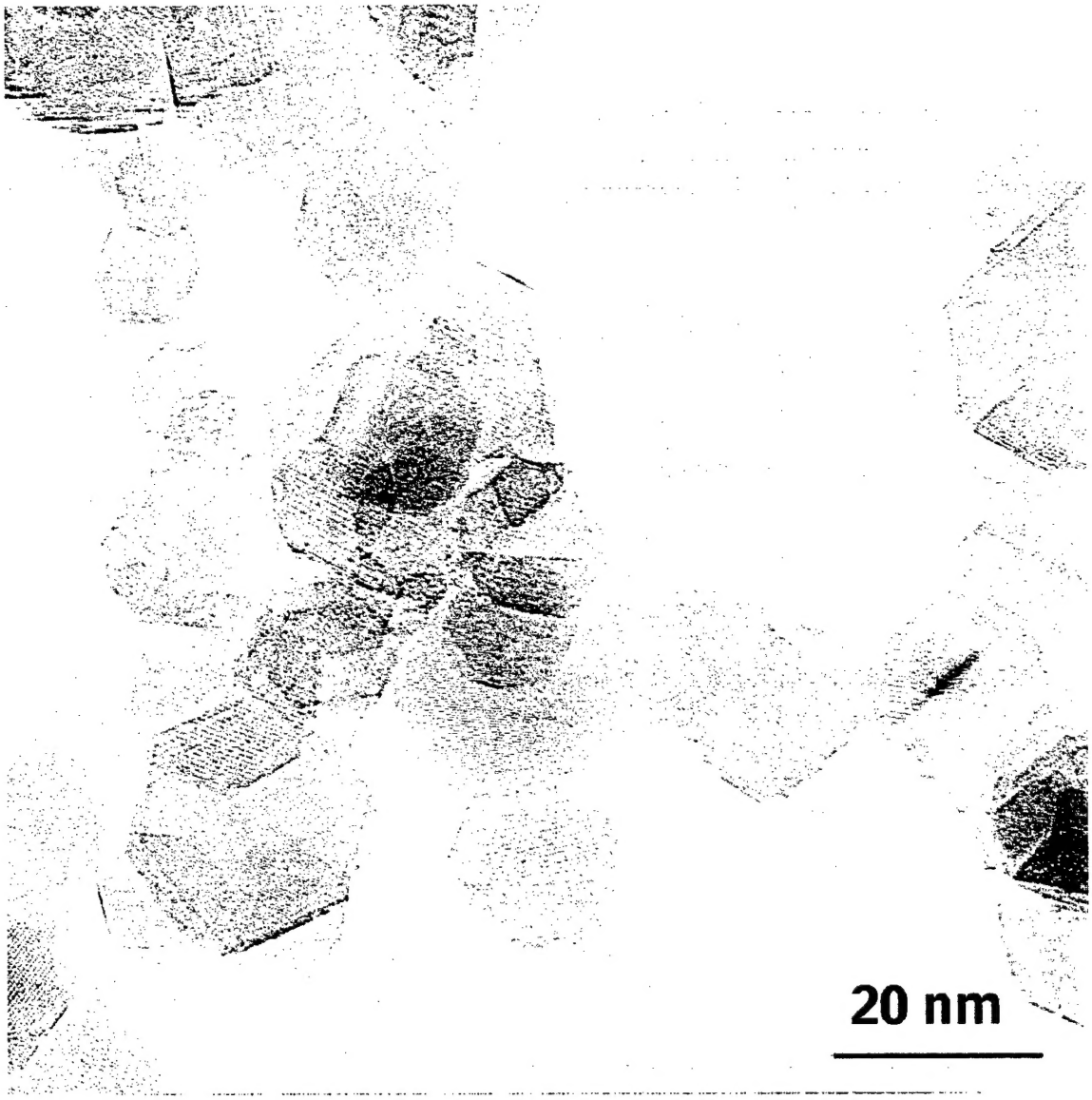


Figure 1. TEM micrograph of alumina nano-particles synthesized by flame spray pyrolysis of metallo-organic precursors soluble in alcohol.

$Pr^{3+}$:β"-$Al_2O_3$, and $Gd^{3+}$:δ-$Al_2O_3$. In the visible spectral region, UV-transmitting, fused silica refractive lenses was used to collect and image light emitted from the powder on the entrance to the spectrometer and a R955 photomultiplier was used for detection. For infrared work, because off-axis reflective optics was not available to collect signal light, IR-transmitting $CaF_2$ lenses were used to match the light collection optics to the spectrometer focal length, and a nitrogen-cooled EG&G J10D HgCdTe detector was positioned at the exit slit.

Experiments involving excitation of $Tm^{3+}$:δ-$Al_2O_3$ nanopowders with an optical beam were also undertaken. Thulium has absorptive transitions in the 800 nm region that overlap the output range of Ti:sapphire lasers. Hence with our available laboratory sources we were able to scan through the near IR spectral region (770-850 nm) and observe three main upconversion lines from $Tm^{3+}$. Upconversion emission generally results from multi-photon dynamics within individual rare earth ions, or from multi-atom dynamics occurring within coupled ion clusters. Upconversion mechanisms are potentially sensitive to changes in the non-radiative decay within nanosystems. So, the thrust of these measurements was to look for differences between the excitation/emission spectra of alumina nanopowders and those found in single crystals, with which we have extensive experience.

Measurements of the transport mean free path l* in our samples were also made, using coherent back-scattering (CBS). Apparatus used in preliminary experiments was completely rebuilt to improve angular resolution and to implement computer control not only of data acquisition but of polarization modulation and scanning control. Two CBS setups were assembled - one based on a rotating detector geometry and one based on a rotating sample geometry - to provide independent experimental determinations of l* from observations of the back-scattering cone. Together with the introduction of an electronically-variable polarization rotator, these improvements provide all possible combinations of incident and exiting polarizations - to furnish a thorough tensorial characterization of wave transport conditions in our powders. Measurements so far however have only determined l* at three different wavelengths. Additional experiments are planned for all possible polarization combinations at nearly two dozen wavelengths to be provided by Ar, dye and Ti:sapphire lasers. This will provide a much more thorough exposition of the scattering behavior of our samples, as evidenced by l* values, at optical wavelengths.

Electron trajectory simulations were run on a workstation to compare electron penetration distances in alumina with the experimentally determined values of l*. It is important to compare calculated penetration depths and measured l* values because serious limitations to the efficiency of generation and extraction of optical energy will arise in nanopowders if these quantities are not of the same order. The ease of experimentation and prospects for useful applications depend on the practicality of using electrons to generate light at depths within the medium from which it can escape. Average penetration depths of electrons in alumina were therefore calculated using a CASINO algorithm [1] that computes classical trajectories for electrons of specified energies in materials of specified

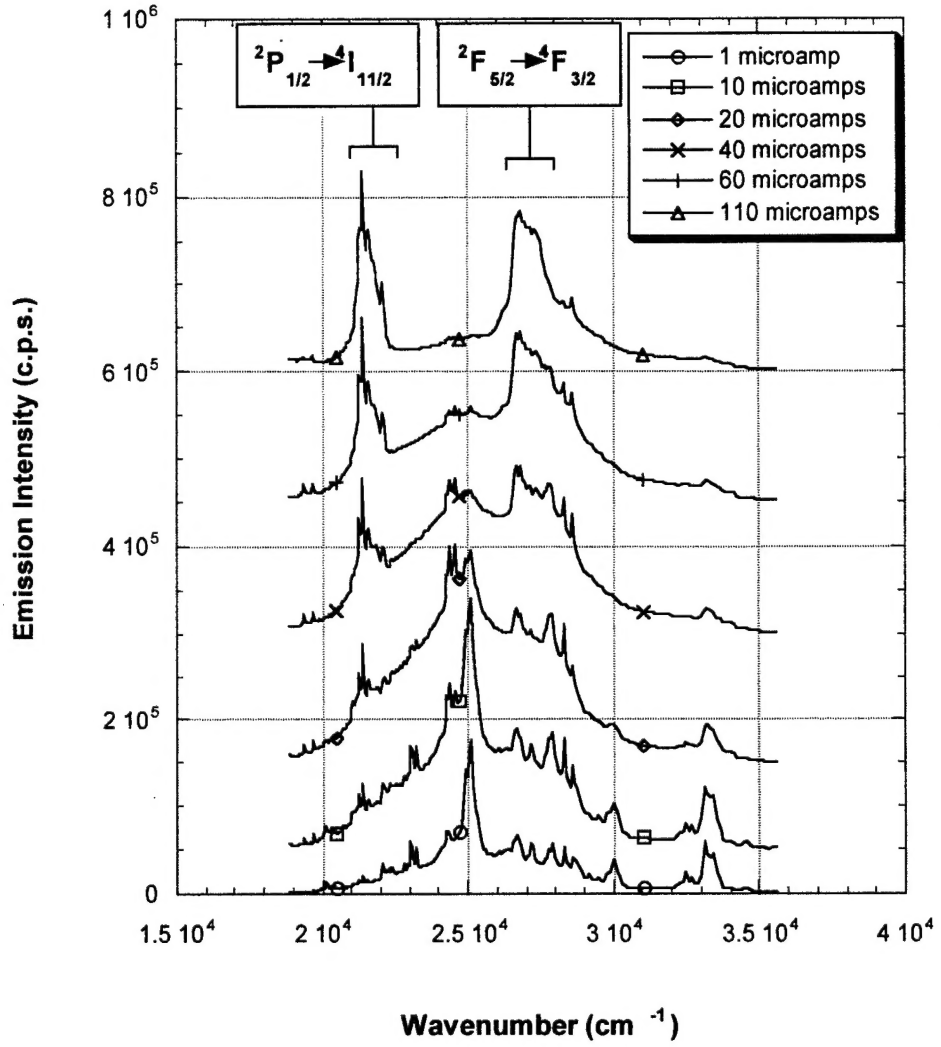


Figure 2. Cathodoluminescence spectra of $Nd^{3+}$:δ-$Al_2O_3$ excited at various current levels with 7 keV electrons in ultrahigh vacuum.

density and scattering cross section. Mott scattering cross sections were used because of the low energy range of our experiments. The CASINO program was modified to calculate penetration depths taking the filling fraction of the alumina powder into account, and the results were quite helpful in interpreting observations of stimulated emission thresholds. They are compared with the results of our initial experiments in the next section.

## III. Results

At the outset, optical emission spectra were recorded at different electron currents in the most readily accessible spectral region where sensitive detectors are available to facilitate the recording of weak luminescence signals. For this we examined electron-pumped luminescence from a sample of $Nd^{3+}$:$\delta$-$Al_2O_3$. In Fig. 2, numerous emission lines from $Nd^{3+}$ are evident throughout the UV and visible spectral regions, and they undergo remarkable changes as the current is increased. By examining the spectroscopic assignments of lines in the neighborhood of 300-370 nm, it was possible to conclude that emission from the $^2F_{5/2}$ state was quenched on all transitions to lower states save one, the $^2F_{5/2}$ - $^4F_{3/2}$ transition, at current levels >40 ($\mu$A). An example of such a quenched feature originating from $^2F_{5/2}$ is the line at 32,500 $cm^{-1}$. The disappearance of emission lines which have the same upper state ($^2F_{5/2}$) as a transition which grows in intensity constitutes direct evidence of population inversion in the $^2F_{5/2}$ state. This result was a significant step in meeting one critical objective of this project - namely to establish that continuous-wave gain can be achieved in electrically-pumped nanophosphors at optical wavelengths.

Identical quenching behavior was observed for another state in the Nd samples. Emission on the $^2P_{1/2}$ -$^4I_{11/2}$ transition grew in intensity above a sharp "threshold" value of electron current, as shown in Fig. 3. At 10 $\mu$A, all other emission lines originating from the $^2P_{1/2}$ state disappeared. An example of a quenched line is the feature at 23,000 $cm^{-1}$. Because the output curves have different slopes above and below the threshold point, and are linear above and below this point, they provide direct evidence of electrically-pumped, continuous-wave laser action in Nd powder at room temperature.

Next, efforts were directed to similar experiments on Pr, Ce and Gd-doped powders identified as candidates for MIR laser action. Evidence of laser action and MIR emission was sought first in Pr:$\delta$-$Al_2O_3$. A series of spectra obtained at electron beam voltages between 1-4 keV showed more striking threshold behavior in the visible spectral range than in Nd powders. Representative data is shown in Fig. 4. For this dopant, no obvious quenching behavior was observed among the components of the red visible emission lines near 630 nm, probably because of the limited spectral involvement of different manifolds over this narrow range. Emission signals were sought at 3 microns with this sample in the chamber, but not observed. Alignment difficulties caused by the use of refractive, rather than reflective, optics reduced signal-to-noise ratios below unity. This was confirmed during a search for 1.7 micron emission on the $^5D_3$ - $^5D_4$ transition in Tb reference powder. During these scans, the second order of $^5D_4$ - $^7F_6$ green emission was observed with an intensity nearly one thousand times smaller than expected. Low

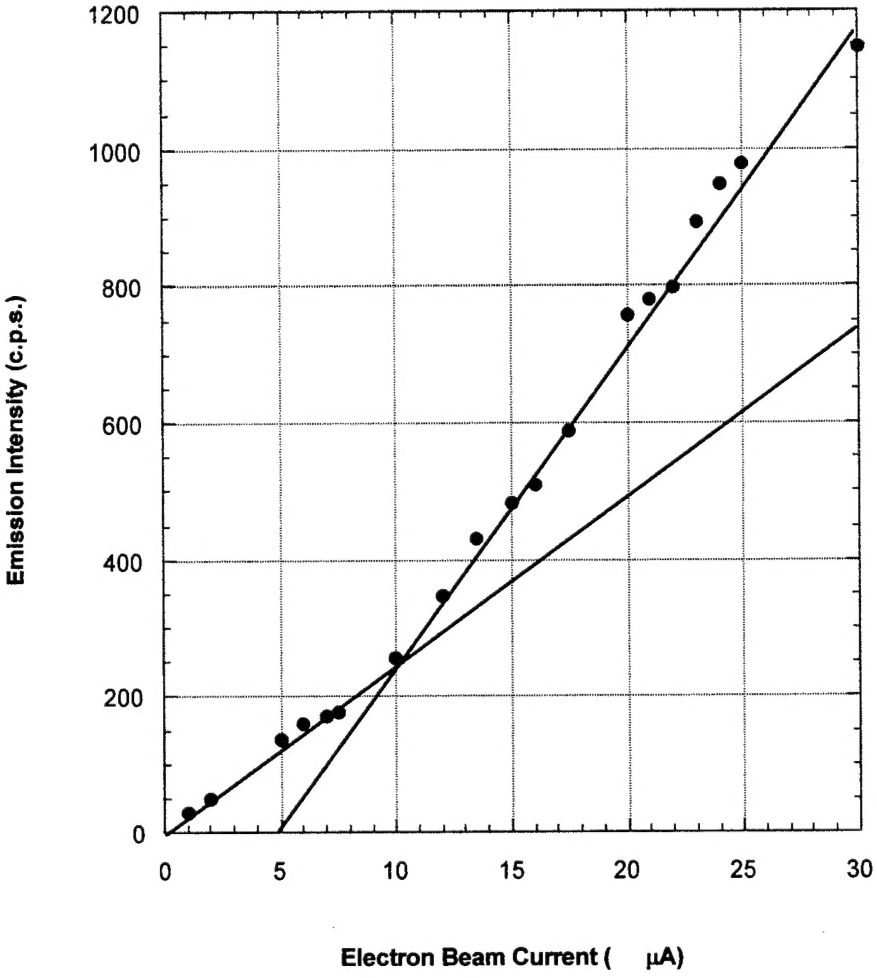


Figure 3. Cathodoluminescent intensity versus current in a sample of n-Nd:alumina, showing two linear output regimes separated by an abrupt transition at a current of 10 μA.

signal-to-noise was traced to a combination of axial misalignment and chromatic aberrations in the refractive optics train. As part of our continuing research on this project, alignment problems will be solved by the introduction of purely reflective, off-axis collection optics and pre-alignment of the spectrometer with a 3.39 micron He-Ne laser source.

Ce powders yielded ultraviolet laser action near 360 nm. The bandwidth of the emitted light in this case was exceptionally broad because of the inter-configurational nature of the observed optical transition. Results with Ce-doped powders have been fully disclosed in publications [2-4] appended to this report. Hence they will not be discussed further here.

Cathodoluminescence of Gd:δ-alumina was also analyzed. As shown in Fig. 5, some of the expected short wavelength emissions were observed immediately. In the figure, the $^6P_{3/2}$ - $^8S_{7/2}$, $^6P_{5/2}$ - $^8S_{7/2}$, and $^6P_{7/2}$ - $^8S_{7/2}$ ultraviolet lines appear, but their intensities saturated so quickly at low currents that the shape of the output curve could not be reliably deduced. Equipment limitations at low current levels thus made it very difficult to provide any convincing evidence of population inversion in these samples, based on observations in the UV-VIS region. The tendency to saturate is undoubtedly due to the extended lifetimes of the $^6P_{7/2}$ excited state of Gd, which has a large energy gap with respect to the next lowest state - namely the ground state - and is spin-forbidden to decay radiatively to ground. The absence of $^6I_{7/2}$ - $^8S_{7/2}$ transitions in the emission spectrum of Fig. 5 probably indicates fast radiative relaxation of the proposed upper state of the Gd MIR laser. This is a very promising finding. It could mean that MIR laser conditions have already been achieved in this sample with electrical pumping. However, low signal-to-noise ratio in the 3-5 micron region incurred by the use of refractive optics and a very high dispersion grating in our current apparatus prevented us from confirming this important result. It remains to be seen whether the MIR radiation from Gd nanopowders can be directly detected through the implementation of reflective collection optics at lower dispersion.

So far, all measurements of the transport mean free path l* made in our samples using coherent back-scattering (CBS) by two independent techniques have confirmed sub-wavelength propagation distances in our samples. CBS measurements have provided a total of three determinations of l* at optical wavelengths in samples exhibiting laser properties similar to those displayed in Figs. 1 and 2. The value of l* was invariably found to be lower than $\lambda/2$, making these among the shortest values ever reported for lossless elastic scattering at optical frequencies. The results of measurements at three laser wavelengths between 300 and 900 nm are shown in Fig. 6, addressing in a preliminary way our objective to evaluate transport conditions and to search for indicators of strong localization over the broadest possible wavelength range during this project.

Finally, the numerical simulations that we performed with a modified CASINO algorithm provided a basis for comparison of electron penetration distances in alumina with the

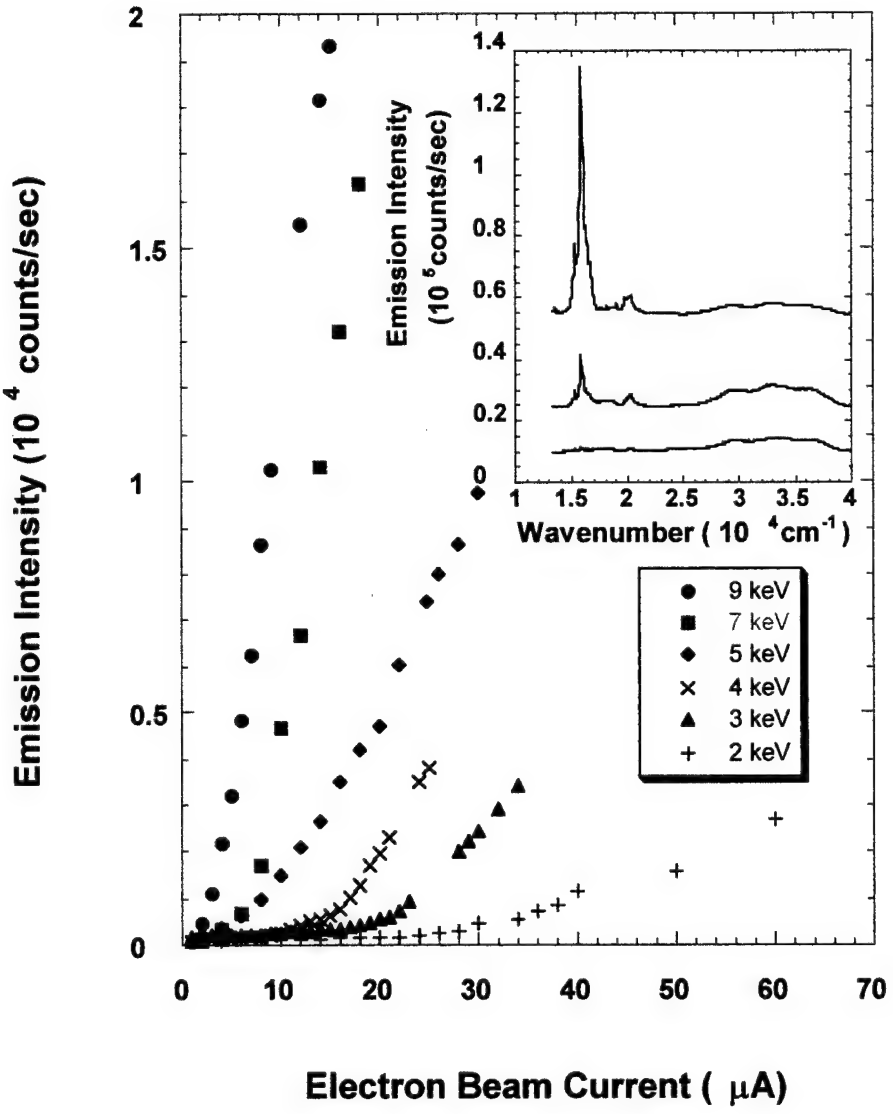


Figure 4. Optical emission at 633 nm in Pr:δ-Al2O3 at room temperature. Note the pronounced thresholds at low voltages (1-4 keV), and linear output above threshold for the same curves.

experimentally determined values of l*. This comparison was a key materials-related objective identified in our technical proposal. In Fig. 7, results of the simulations for average penetration depths of electrons in alumina are shown for various energies of the incident particles for a volume filling fraction of approximately 0.5. In the range 1-5 keV, it is important to note that the penetration depths in δ-alumina are of the same order as experimentally-determined l* values (Fig. 5), and that they depend systematically on voltage. This implies that electron energy deposition can be adjusted within a range that will allow energy deposition to be matched with the size of the gain volume for efficient stimulated emission.

Cathodoluminescence experiments in Pr-doped samples were performed at several different voltages and revealed an important dependence of laser threshold on incident electron energy. In Fig. 5, luminescent curves at voltages in the range 1-4 keV show rather dramatic thresholds that vary significantly with electron energy. For higher voltages, lower thresholds were observed. At voltages above 5 keV, where the electron penetration exceeded the average optical transport distance, the emission curves developed more curvature and thresholds became indistinct. Monte Carlo simulations performed with the CASINO PIC-code for the alumina powder densities of our experiments (Fig. 6) provided accurate penetration depths R for the various voltages, for comparison with the optical transport distance $l^*(\lambda)$ determined at experimental wavelengths. Interestingly, it was found that the lowest, most distinct thresholds were obtained when R was approximately equal to l*. Consequently, we found consistency with the idea that an intermediate deposition depth would optimize the efficiency of electrically-pumped random lasers.

Finally, a limited number of l* determinations were made at different optical wavelengths, in an effort to estimate the breadth of the spectral region over which strong scattering feedback can be expected to mediate laser action of the type reported here. The results are shown in Fig. 7, where the solid curve is merely a guide to the eye based on the idea that even in the strong scattering regime a Rayleigh-like dependence ($\sim\lambda^4$) may persist in the variation of mean free transport distance l* with wavelength. The data indicate that the spectral region may be very wide indeed, possibly extending over the entire UV-VIS-NIR range. This wide range will facilitate additional experiments, particularly ones on trapping of light and enhancement of energy transfer processes within finely powdered solids [5].

## IV. Summary

Continuous-wave laser emission in δ-alumina nanopowders doped with several different types of rare earth ion was achieved for the first time during year one of this project. Stimulated emission was observed at ultraviolet (Ce 363nm), visible (Nd 470, Pr 633 nm) and near infrared wavelengths, as evidenced by dramatic spectral quenching and intensity thresholds in emission. These results have been described in numerous publications and conference proceedings, some of which are appended to this report. Preliminary, indirect evidence was found for a rapid emission in one candidate MIR powder laser system, but

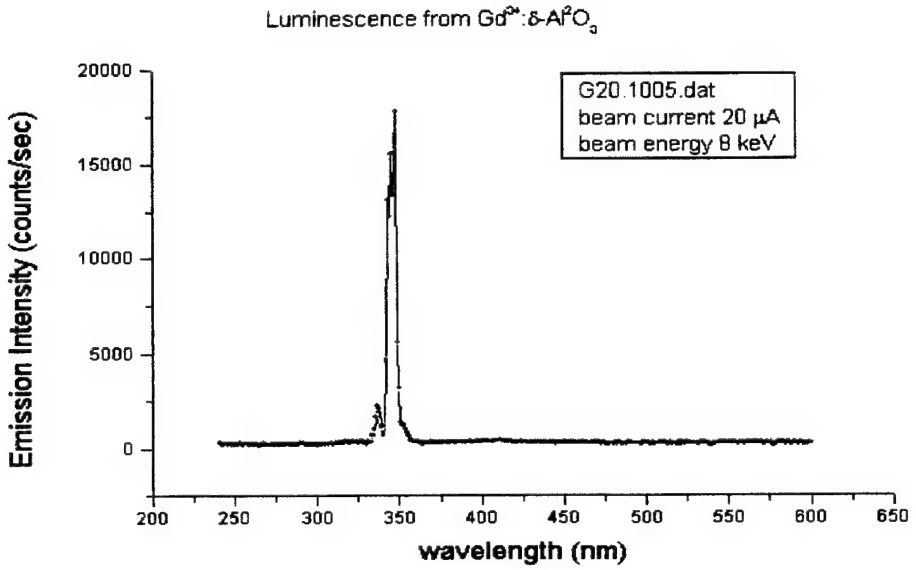


Figure 5. Ultraviolet luminescence spectrum of Gd:alumina at room temperature, excited by an electron beam in ultra-high vacuum at a current of 20 μA and an accelerating voltage of 8 keV. Three transitions originating from the $^6P$ states of Gd are evident.

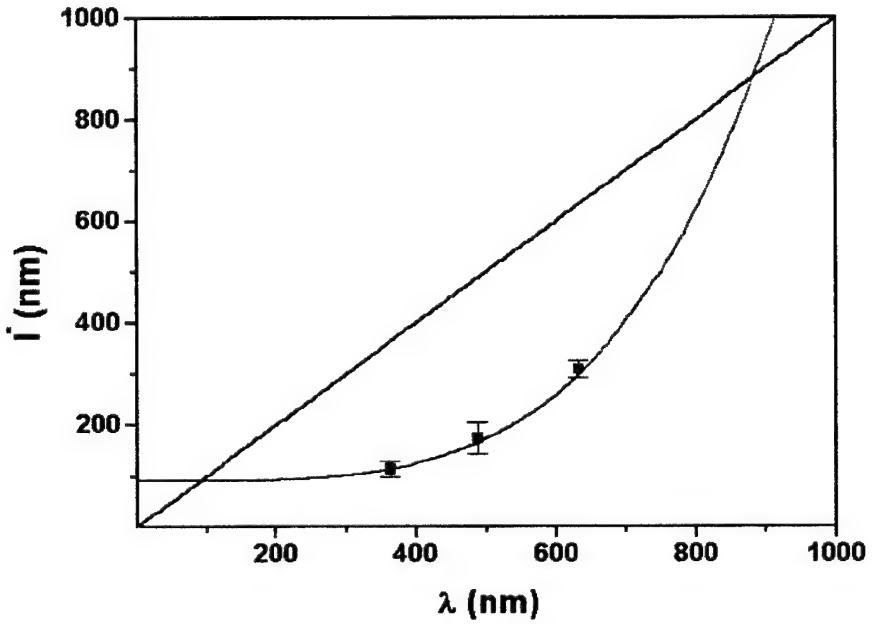


Figure 6. Experimental values of mean free transport distances l* for light in nanoalumina, as derived from CBS observations. Polarization of the incident light was perpendicular to the scanning plane, making the data points upper limits on l* at the indicated wavelengths.

the associated 3-5 micron radiation was not directly detected due to experimental difficulties and confirmation of laser action in this extreme wavelength range could not be made. In the midinfrared, the strong scattering feedback necessary for the successful operation of cw powder lasers is expected to be difficult to achieve since the Rayleigh scattering probability falls off with the fourth power of wavelength. Further work in this wavelength range will require special experimental approaches. Fortunately, in addition to the guidance provided by these initial experimental results at short wavelengths, analytic theory [2] was developed by us for the prediction of system properties necessary to shift strong localization to the longer wavelength range of the midinfrared. This will be very helpful in guiding new efforts to synthesize powders with properties appropriate for midinfrared applications.

**References:**

1. R. Gauvin, P. Hovington, D. Drouin, Scanning 19, 1-14(1997); ibid, pp. 20-28; ibid, pp. 29-35.

2. S.C. Rand, "Strong localization of light and photonic atoms", Can. J. Phys. 78, 625(2000).

3. R.M. Laine, T. Hinklin, G. Williams, and S.C. Rand, "Low-cost nanopowders for phosphor and laser applications by flame spray pyrolysis", Mat. Sci. Forum 343-346, 500(2000).

4. G. Williams, S.C. Rand, T. Hinklin, and R.M. Laine, "Laser action in strongly scattering rare-earth-doped dielectric nanophosphors", Phys. Rev. Lett. (submitted).

5. S. Redmond and S.C. Rand (invited), "Localization and trapping-mediated phenomena in dense nanopowders", Symposium on New Developments in Strong Scattering, Annual Meeting of the Optical Society of America, Long Beach, California (2001).

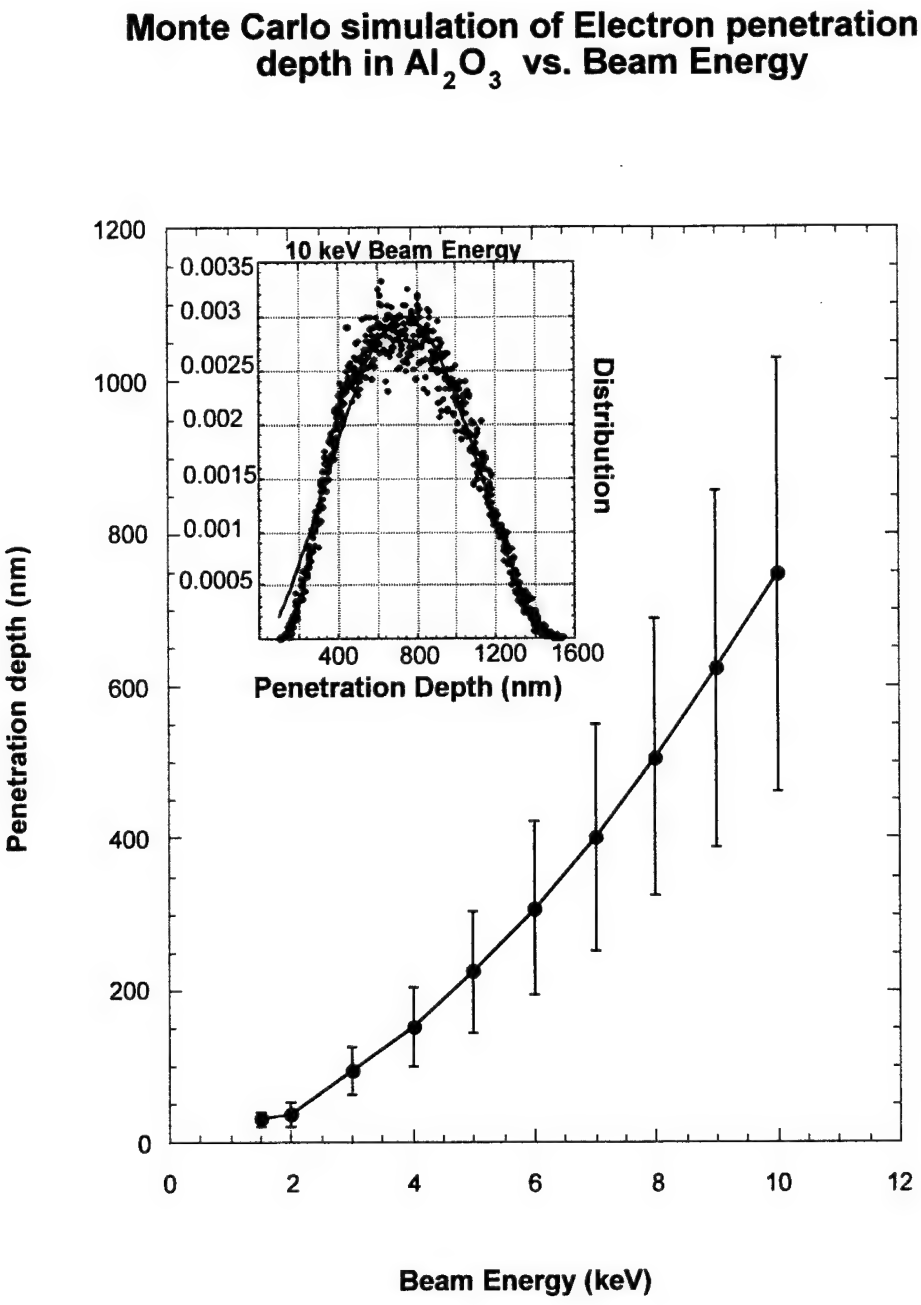


Figure 7. Simulation of electron penetration depths in alumina, based on the CASINO algorithm. Each point is the result of many trajectory calculations for a given electron energy. These calculations generate a curve similar to the inset, which illustrates the distribution obtained in this way for 10 keV.

**List of**
**Publications & Conference Proceedings**

## Publications & Conference Proceedings


1. G. Williams, S.B. Bayram, S.C. Rand, T. Hinklin, and R.M. Laine, "Laser action in strongly scattering rare-earth-doped dielectric nanophosphors", Phys. Rev. Lett. (submitted).

2. S.C. Rand, "Strong localization of light and photonic atoms", Can. J. Phys. 78, 625(2000).

3. R.M. Laine, T. Hinklin, G. Williams, and S.C. Rand, "Low-cost nanopowders for phosphor and laser applications by flame spray pyrolysis", Mat. Sci. Forum 343-346, 500(2000).

4. R. M. Laine, T. Hinklin, G. Williams, S.C. Rand, "Low-Cost Nanopowders for Phosphor and Laser Applications by Flame Spray Pyrolysis," in the Proc. of ISMANAM-99, Scitec & Trans Tech. Publ., Zurich, Switzerland, September 1999 (in press).

5. S.C. Rand, G. Williams, T. Hinklin, R.M. Laine, "Laser Phosphors", Fifth Int. Conf. on the Science and Technology of Display Phosphors, San Diego, Nov. 8-10(1999), paper 8.2.

6. S.B. Bayram, T. Jiang, S. Redmond, G. Williams, and S.C. Rand, "Wavelength Dependence of Optical Transport in Strongly Localizing Rare Earth Media", Qu. Elect. & Laser Spectr. Conf. (QELS 2000), San Francisco, May 7-12, 2000, paper JMB7.

7. Rare earth-doped, oxide single crystal nanoparticle formation, Tom Hinklin and Richard M. Laine, Proc. of American Ceramic Society, Indianapolis, IN, April 30, 1999.

8. Continuous-wave laser action from Lanthanide doped nanoalumina powders, T. Hinklin, R. M. Laine, S. Rand, and G. Williams, Thermal Spray processing of Nanoscale Materials II Quebec City, August 15-20 1999.

9. Continuous-wave laser action from Lanthanide doped nanoalumina powders, T. Hinklin, R. M. Laine, S. Rand, and G. Williams, MRS (Materials Research Society)Fall 99 Boston MA December 2, 1999

10. Continuous-wave laser action from Lanthanide doped nanoalumina powders, synthesis and properties, R. M. Laine, T. Hinklin, S. Rand, and G. Williams, MRS (Materials Research Society)Fall 99 Boston MA December 2, 1999.

11. Continuous-wave laser action from Lanthanide doped nanoalumina powders, synthesis and properties, R. M. Laine, T. Hinklin, S. Rand, and G. Williams, American Ceramic Society (ACerS 2000), St. Louis MO, May 3, 2000.

**Publications & Conf. Proceedings** (Cont'd):

12. Ceria-doped, delta alumina: synthesis, characterization and morphological evolution, T. Hinklin and R. M. Laine, ACerS (American Ceramic Society) 2000, St. Louis MO, May 3, 2000.

13. S. Redmond and S.C. Rand (invited), "Localization and trapping-mediated phenomena in dense nanopowders", Symposium on New Developments in Strong Scattering, Annual Meeting of the Optical Society of America, Long Beach, California (2001).

# APPENDIX

Reprints of Published Papers